Hindawi
Wireless Communications and Mobile Computing
Volume 2021, Article ID 4342983, 10 pages
https://doi.org/10.1155/2021/4342983

Research Article

Enabling Device-to-Device Transmission for NOMA-Aided Systems

Anh-Tu Le,[1] **Nhan Duc Nguyen**,[2] **Dinh-Thuan Do**,[3] **and Munyaradzi Munochiveyi**[4]

[1]*Faculty of Electronics Technology, Industrial University of Ho Chi Minh City (IUH), Ho Chi Minh City 700000, Vietnam*
[2]*Innovation Center, Van Lang University, Ho Chi Minh City, Vietnam*
[3]*Department of Computer Science and Information Engineering, Asia University, Taichung 41354, Taiwan*
[4]*Electrical and Electronics Engineering Department, University of Zimbabwe, Mount Pleasant, Harare, Zimbabwe*

Correspondence should be addressed to Nhan Duc Nguyen; nhan.nd@vlu.edu.vn

Received 14 August 2021; Accepted 16 October 2021; Published 16 November 2021

Academic Editor: Vinayakumar Ravi

To utilize the close transmission, we assume that the device-to-device (D2D) link is activated to improve the performance of the far user. We consider two groups of users in the nonorthogonal multiple access- (NOMA)- aided wireless system. These features are necessary for massive connectivity in future wireless systems. The system performance also shows suitable performance at far distance users. To evaluate the performance in detail, we derive novel closed form expressions of outage probability. In practical situations impaired by channel uncertainty, it is necessary to evaluate the impact of channel error levels on outage probability. Our numerical results indicated that the transmit power at the base station and channel error level are the main impacts on system performance. Despite these impacts, our obtained numerical results demonstrated that the proposed scheme can still increase energy efficiency and achieve significant outage performance via many practical challenges.

1. Introduction

1.1. Motivation. Since spectral efficiency and massive connectivity are the main requirements in the fifth generation (5G) networks, and the applications of nonorthogonal multiple access (NOMA) have drawn lots of studies [1–3]. Further, NOMA is considered as a simple way to improve energy efficiency [4, 5]. NOMA allows multiple users to be served at the same frequency and time by superimposing a larger number of users in the power domain at the transmitter. Different from conventional orthogonal multiple access (OMA), the receiver of NOMA acquires successive interference cancellation (SIC) in its detection operation [6, 7]. In the NOMA system, by examining channel conditions (the near user and the far user), the users are divided into different orders of signal detection. The authors in [8] raised the influence of signal processing of the near user to the far user. To ensure user fairness, a power allocation scheme needs to be designed for NOMA users. In particular, more power is assigned to the far user with poor channel condition while less power is assigned to the near user with good channel condition. Recently, to achieve a balance between the performance of two users, NOMA is jointly designed with cooperative techniques. In a cooperative NOMA system, the performance gaps among these NOMA users can be determined by numerous system parameters such as transmit power at the base station [9–15]. To improve energy efficiency for low-power devices, [16] proposed a wireless power transfer paradigm for cooperative NOMA networks. To forward the signal to the far user, the near user can harvest energy from the source node.

Moreover, in [17, 18], the authors proposed the utilization of NOMA in device-to-device (D2D) communication networks. Numerous authors considered using NOMA to enhance D2D in different scenarios. Below, we present some noteworthy examples such as in [19], and the authors considered maximizing the D2D system sum rate by jointly optimizing the subchannel of D2D groups and the power allocation of receivers in each D2D group. In [20], the authors considered a NOMA-aided full-duplex (FD) D2D system. The authors analyzed the outage probability (OP) performance of the system NOMA weak and

strong users. In [21], the authors studied the combination of NOMA and mobile edge computing (MEC) in D2D systems. The authors proposed different algorithms to solve the joint optimization problem of computing resource, power, and channel allocations to minimize the weighted sum of the energy consumption and user delay. In [22], the authors investigated the energy efficiency maximization associated with underlaying NOMA enabled D2D systems. In [23], the authors considered the OP and power control of an unmanned aerial vehicle-(UAV-) enabled D2D underlaying NOMA systems.

Continuing, in [24], the authors maximized the sum rate of D2D user pairs while maintaining the rate requirements of NOMA-based cellular users in D2D underlaying NOMA-based cellular systems. In [25], the authors proposed NOMA to enhance the spectral efficiency of D2D-assisted cooperative relaying system (CRS). The authors demonstrated via simulation results that for D2D-assisted CRS utilizing NOMA with power allocation improved the achievable rate significantly compared to traditional CRSs relying on NOMA and without NOMA. In [26], the authors maximized the sum rate of underlay D2D users aided by NOMA by jointly designing user clustering and power assignment. In [27], the authors considered beamforming in multiuser multiple-input multiple-output (MU MIMO) downlink cellular network with NOMA-aided D2D users. In [28], the authors proposed an interference aware scheme for cooperative hybrid automatic repeat request-(HARQ-) aided NOMA system for massive D2D networks. The authors in [29] considered the secrecy outage probability (SOP) and OP for NOMA-enabled cooperative D2D systems in the presence of an eavesdropper as well as quality-of-service (QoS) provisioning. In [30], the authors studied covert communications in D2D underlay-aided power-domain NOMA. The authors noted that due to D2D devices being power limited, it is easy for them to be comprised easily by adversaries. Hence, it's essential to enable D2D communication links to transmit covert signals to guarantee a low probability of detection.

2. Related Works

So far in this discussion, we have considered several NOMA-aided D2D networks with perfect channel state information (CSI). Differently, in [31], the authors integrated FD relaying and time splitting simultaneous wireless information and power transfer (SWIPT) into D2D networks to address bandwidth and energy losses in conventional D2D networks with half-duplex relays and limited energy storage capability. The authors derived ergodic capacity expressions and closed form OP with imperfect CSI conditions. In another work on D2D networks powered by SWIPT in [32], the authors studied the resource allocation problem in NOMA-enabled D2D systems with SWIPT under imperfect CSI conditions. Here, the authors modeled the problem as a nonconvex optimization problem where the transmit power, power splitting factor, and resource block assignment factor are jointly designed to obtain the maximum OP of each D2D user, the SIC decoding order, and the maximum transmit power of the base station and D2D users. The authors developed a relaxation approach to transforming the obtained mixed-integer fractional programming problem with intractable OP constraints into a nonprobabilistic problem, and then the variable substitution and Dinkelbach's approach are used to transform the nonprobabilistic problem into a nonconvex one. Then, an energy-efficiency-based iterative algorithm is utilized to solve the intractable OP constraints. Recent work in [33] considered power efficient secure FD-aided SWIPT in NOMA-enabled D2D networks with imperfect CSI. The authors studied the system total transmit power minimization and formulated a multiobjective optimization (MOO) problem utilizing the weighted Tchebycheff method. The authors used a set of linear matrix inequalities (LMI) to transform the nonconvex constraints into convex constraints. Also, the authors utilized a bounded transmit beamforming vector design with artificial noise (AN) to satisfy robust power allocation in the presence of an eavesdropper with imperfect CSI.

In [34], the authors considered two-stage power allocation in maximizing the system sum rate of a cooperative NOMA-aided D2D system operating with imperfect CSI at the base station. In [35], the authors also proposed a power allocation algorithm for D2D-assisted cooperative NOMA networks under imperfect CSI. The authors converted the probabilistic nonconvex optimization problem into a nonprobabilistic nonconvex optimization problem solved via successive convex programming (SCP). Then, Lagrangian dual multiplier and Karush-Kuhn-Tucker methods are used to iteratively obtain suboptimal power allocation coefficients. In [36], the authors considered the integration of NOMA-aided D2D communication with fog computing (FC) under imperfect CSI to enhance the spectral efficiency of mission critical applications such as internet-of-medical-things (IoMTs), UAVs, and autonomous vehicles as well as secrecy capacity via coalition game theory. In [37], the authors considered millimeter wave (mmWave) NOMA-aided D2D systems under transceiver hardware and CSI impairments. The authors derived generalized OP expressions and confirmed via simulation results that their proposed system outperforms OMA.

3. Contributions

Motivated by the above, this article considers the closed form OP expressions of groups of users in D2D-enabled NOMA transmissions under imperfect CSI. Differently from the work in [37], we design our NOMA-aided D2D system model to follow a radial approach commonly found in cellular networks with the base station located in the center of the network. Also, unlike [28], which considered large scale NOMA-assisted D2D networks under perfect CSI conditions, in this work, we consider such networks under imperfect CSI conditions. Then, based on the stochastic geometry approach, we investigate the impact of channel estimation error on OP and throughput of the proposed system. Table 1 provides a comparison of this work versus the past studies in [31–37].

Our contributions are listed as follows:

(i) We consider transmission assisted by NOMA where a single antenna base station communicates with two groups of D2D users arranged in a radial manner around the base station. We study the case of imperfect

Table 1: A comparison of existing works on NOMA-aided D2D networks with imperfect CSI.

Scheme	Reference	Major contributions
FD-SWIPT NOMA-D2D	[31]	The authors derived ergodic capacity expressions and closed form OP with imperfect CSI conditions.
SWIPT NOMA-D2D	[32]	The authors studied the resource allocation problem by modeling the problem as a nonconvex optimization problem where the transmit power, power splitting factor, and resource block assignment factor are jointly designed to obtain the maximum OP of each D2D user, the SIC decoding order, and the maximum transmit power of the base station and D2D users.
Secure FD-SWIPT NOMA-D2D	[33]	The authors studied the system total transmit power minimization and formulated a multiobjective optimization (MOO) problem utilizing the weighted Tchebycheff method.
NOMA-D2D	[34]	The authors considered two-stage power allocation in maximizing the system sum rate of a cooperative NOMA-aided D2D system operating with imperfect CSI at the base station.
NOMA-D2D	[35]	The authors proposed a power allocation algorithm for D2D-assisted cooperative NOMA networks under imperfect CSI.
Fog computing NOMA-D2D	[36]	The authors considered the integration of NOMA-aided D2D communication with fog computing (FC) under imperfect CSI and utilized coalition game theory to enhance spectral efficiency and secrecy capacity.
mmWave NOMA-D2D	[37]	The authors considered mmWave NOMA-aided D2D systems under transceiver hardware and CSI impairments. The authors derived generalized OP expressions and confirmed via simulation results that their proposed system outperforms OMA.
NOMA-D2D	Our work	We consider transmission assisted by NOMA where a single antenna base station communicates with two groups of D2D users arranged in a radial manner around the base station. Then, based on the stochastic geometry approach, we investigate the impact of channel estimation error on OP and throughput of the proposed system. Simulations show that our proposed system still enhances spectral efficiency despite imperfect channel estimation and throughput limitations.

channel estimation to determine the downlink OP performance under Rayleigh fading channels

(ii) We determine the signal-to-interference-plus-noise ratios (SINRs) of the D2D grouped devices and then use them to formulate exact OP formulas over Rayleigh fading channels. The derived expressions are validated by Monte Carlo simulations

(iii) We analyze and compare the OP under various conditions. In particular, we find that transmit power at the base station and channel error are the main impacts on system outage performance. Despite these impacts, our obtained numerical results demonstrated that the proposed scheme can still increase energy efficiency and achieve significant outage performance via many practical challenges

(iv) Also, we note the influence of imperfect channel estimation on the throughput performance. We discover that the imperfect channel estimation impacts SIC which then imposes a ceiling on the throughput rate. This is one of the limitations of the present work. Hence, differently from past studies as seen in [31–37], the obtained simulation results of this work further demonstrate the impact of channel estimation on OP and throughput

The rest of this paper is organized as follows. Section 2 describes the downlink NOMA under Rayleigh channels in D2D networks with imperfect CSI. In Section 3, we consider the scenario of NOMA in terms of outage performance. In Section 4, we consider throughput. In Section 5, we provide extensive numerical simulations, and Section 6 concludes the paper.

4. System Model

The NOMA-aided D2D communication is studied, as shown in Figure 1. This system consists of a base station (S), and two groups of randomly deployed users A_n and B_n. Following the distances from users to S, B_n is considered as the near user, and B_n is within disc D_B with radius R_{D_B}. At longer distances, user A_n is the far user and is within disc D_A with radius R_{D_A}, conditioned on $(R_{D_A} > R_{D_B})$.

The source node S wants to send signals x_{A_n} and x_{B_n} to NOMA users An and Bn, respectively. We denote q_{n_1} and q_{n_2} as the corresponding power allocation coefficients with $|q_{n_1}|^2 + |q_{n_2}|^2 = 1$. In addition, d_{A_n}, d_{B_n}, and d_{C_n} are the distance from S to A_n, S to B_n, and Bn to An, respectively. To conduct performance analysis, we treat h_{SA_n}, h_{SB_n}, and h_{BA} as the channels for links S-A_n, S-B_n, and B_n-A_n, which follow Rayleigh fading channels. In this paper, we examine the impact of the channel estimation error [38] on system performance, and the considered channel is given by

$$h = \widehat{h} + \tilde{h}, \tag{1}$$

where $\widehat{h}$ stands for the estimated fading channel coefficient,

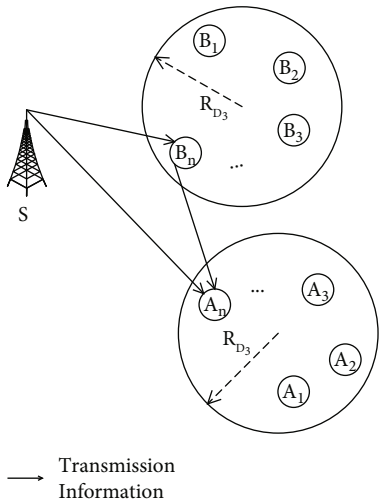

Figure 1: Device-to-device transmission for NOMA-aided systems.

$\tilde{h}$ represents as the error fading channel coefficient with $CN(0, \tilde{\sigma}^2)$, and $\tilde{\sigma}^2$ is constant [39].

In the first time slot, the source node S simultaneously transmits the message $q_{n_1}x_{A_n} + q_{n_2}x_{B_n}$ to users A_n and B_n [16].

Then, the received signal at A_n is given as

$$y_{Sk} = \sqrt{\frac{P_S}{1 + d_k^l}}\left(q_{n_1}x_{A_n} + q_{n_2}x_{B_n}\right)\left(\widehat{h}_{Sk} + \tilde{h}_{Sk}\right) + n_k, \tag{2}$$

where $k \in \{A_n, B_n\}$, P_S, is the transmit power at S, l is the path-loss exponent, and n_k is the additive white Gaussian noise (AWGN) with $CN(0, \sigma_k^2)$.

Next, the signal to interference plus noise ratio (SINR) at user A_n to decode the own signal x_{A_n} is given by

$$\begin{aligned}\gamma_{SA_n}^{x_{A_n}} &= \frac{P_S\left|h\wedge_{SA_n}\right|^2|q_{n1}|^2}{P_S\left|h\wedge_{SA_n}\right|^2|q_{n2}|^2 + P_S\tilde{\sigma}_{SA_n}^2 + \sigma_{A_n}^2\left(1 + d_{A_n}^l\right)} \\ &= \frac{\rho_S\left|h\wedge_{SA_n}\right|^2|q_{n1}|^2}{\rho_S\left|h\wedge_{SA_n}\right|^2|q_{n2}|^2 + \rho_S\tilde{\sigma}_{SA_n}^2 + 1 + d_{A_n}^l}.\end{aligned} \tag{3}$$

Then, the SINR at user B_n to decode signal x_{A_n} is given by

$$\gamma_{SB_n}^{x_{A_n}} = \frac{\rho_S\left|h\wedge_{SB_n}\right|^2|q_{n1}|^2}{\rho_S\left|h\wedge_{SB_n}\right|^2|q_{n2}|^2 + \rho_S\tilde{\sigma}_{SB_n}^2 + 1 + d_{B_n}^l}. \tag{4}$$

Next, the SNR at user B_n to decode the own signal x_{B_n} is given by

$$\gamma_{SB_n}^{x_{B_n}} = \frac{\rho_S\left|h\wedge_{SB_n}\right|^2|q_{n2}|^2}{\rho_S\tilde{\sigma}_{SB_n}^2 + 1 + d_{B_n}^l}, \tag{5}$$

where $\rho_S = P_S/\sigma_k^2$.

In the second time slot (link D2D), user B_n forwards the signal x_{A_n} to user A_n. Then, the signal at D_q user A_n associated with D2D link is given as

$$y_{Bn}^{x_{A_n}} = \sqrt{\frac{P_{Bn}}{1 + d_{BA}^l}}x_{A_n}\left(\widehat{h}_{BA} + \tilde{h}_{BA}\right) + n_{A_n}, \tag{6}$$

where P_{Bn} is the transmit power at the user B_n.

In this step, the SNR to decode signal x_{A_n} at the user A_n is given by

$$\gamma_{B_n,A_n}^{x_{A_n}} = \frac{\rho_S\left|h\wedge_{BA}\right|^2}{\rho_S\tilde{\sigma}_{BA}^2 + 1 + d_{C_i}^{\alpha}}, \tag{7}$$

where $\rho_S = P_S/\sigma_k^2 = P_S/\sigma_{B_n}^2$ is the transmit SNR at source.

By using select combining (SC) scheme, the SINR at the user A_n is given by

$$\gamma_{A_n,SC}^{x_{A_n}} = \max\left(\gamma_{SA_n}^{x_{A_n}}, \gamma_{B_n,A_n}^{x_{A_n}}\right). \tag{8}$$

We achieve the first metric SNR, which is necessary to compute outage probability. We will examine outage performance in the next section.

5. Outage Performance

5.1. Outage Probability. The users in discs D_A and D_B are assumed to follow the homogeneous Poisson point process. The users are modeled as independently and identically distributed (i.i.d.) points. The point W_k has probability density functions (PDFs) given as

$$f_{W_{A_n}}\left(\omega_{A_n}\right) = \frac{1}{\pi\left(R_{D_A}^2 - R_{D_B}^2,\right)}, \tag{9}$$

$$f_{W_{B_n}}\left(\omega_{B_n}\right) = \frac{1}{\pi R_{D_B}^2}. \tag{10}$$

The outage probability is defined as the probability that the expected SNR is less than the threshold SNR. In particular, the outage probability of the user B_n can be formulated by

$$P_{B_n} = 1 - \Pr\left(\gamma_{SB_n}^{x_{B_n}} > \gamma_2\right). \tag{11}$$

Proposition 1. *The closed form expression of the user B_n is given as*

$$P_{B_n} = 1 - \frac{e^{-\theta_2\left(\rho\tilde{\sigma}_{B_n}^2 + 1\right)}}{R_{D_B}^2\theta_2}\left(1 - e^{-\theta_2 R_{D_B}^2}\right). \tag{12}$$

Proof. With the help of (5), (11) can be rewritten as

$$P_{B_n} = 1 - \Pr\left(\left|h\wedge_{SB_n}\right|^2 > \theta_2\rho\tilde{\sigma}^2_{B_n} + \theta_2\left(1 + d^l_{B_n}\right)\right), \quad (13)$$

where $\theta_2 = \gamma_2/\rho|q_{n2}|^2$.

Then, it can be calculated as

$$P_{B_n} = 1 - \frac{2}{R^2_{D_B}}\int_0^{R_{D_B}}\int_{\theta_2\rho\tilde{\sigma}^2_{B_n}+\theta_2\left(1+d^l_{B_n}\right)}^{\infty} re^{-x}dxdr. \quad (14)$$

By following the result reported in [40], we consider the special case $l = 2$, then, we can express P_{B_n} as

$$P_{B_n} = 1 - \frac{2e^{-\theta_2\rho\tilde{\sigma}^2_{B_n}}}{R_{D_B}}\int_0^{R_{D_B}} re^{-\theta_2\left(1+r^2\right)}dr \quad (15)$$

Based on (3.321.4) in [41], we can obtained (12).

The proof is complete.□ □

Next, the outage probability of the user A_n can be expressed as [42]

$$P_{A_n} = \Pr\left(\gamma^{x_{A_n}}_{A_n,SC} < \gamma_1\right). \quad (16)$$

Proposition 2. *The closed form expression of outage probability for the user A_n is given as*

$$P_{A_n} = \left(1 - \frac{2e^{-\theta_1\left(\rho\tilde{\sigma}^2_{SA_n}+1\right)}\left(e^{-\theta_1R^2_{D_B}} - e^{-\theta_1R^2_{D_A}}\right)}{\left(R^2_{D_A} - R^2_{D_B}\right)\theta_1}\right) \left(1 - \frac{\rho e^{-\gamma_1\tilde{\sigma}^2_{BA}}}{\left(R^2_{D_A} - R^2_{D_B}\right)\gamma_1}\left(e^{-\gamma_1R^2_{D_A}/\rho} - e^{-\gamma_1R^2_{D_A}/\rho}\right)\right). \quad (17)$$

Proof. In this case, we can rewrite (16) as

$$P_{A_n} = \Pr\left(\gamma^{x_{A_n}}_{A_n,SC} < \gamma_1\right) = \underbrace{\Pr\left(\gamma^{x_{A_n}}_{SA_n} < \gamma_1\right)}_{I_1}\underbrace{\Pr\left(\gamma^{x_{A_n}}_{B_n,A_n} < \gamma_1\right)}_{I_2}. \quad (18)$$

With the help of (10), we can rewrite I_1 as

$$I_1 = 1 - \Pr\left(\left|h\wedge_{SA_n}\right|^2 > \theta_1\rho\tilde{\sigma}^2_{SA_n} + \theta_1\left(1 + d^l_{A_n}\right)\right) = 1 - \frac{2}{R^2_{D_A} - R^2_{D_B}}\int_{R_{D_B}}^{R_{D_A}}\int_{\theta_1\rho\tilde{\sigma}^2_{SA_n}+\theta_1\left(1+r^2\right)}^{\infty} re^{-x}dxdr,$$

where $\theta_1 = \gamma_1/\rho(|q_{n1}|^2 - \gamma_1|q_{n2}|^2)$.

Moreover, I_1 can be rewritten as

$$I_1 = 1 - \frac{2e^{-\theta_1\left(\rho\tilde{\sigma}^2_{SA_n}+1\right)}}{R^2_{D_A} - R^2_{D_B}}\int_{R_{D_B}}^{R_{D_A}} re^{-\theta_1r^2}dr = 1 - \frac{2e^{-\theta_1\left(\rho\tilde{\sigma}^2_{SA_n}+1\right)}}{R^2_{D_A} - R^2_{D_B}}\left(\int_0^{R_{D_A}} re^{-\theta_1r^2}dr - \int_0^{R_{D_B}} re^{-\theta_1r^2}dr\right). \quad (20)$$

Similarly, I_1 can be obtained by

$$I_1 = 1 - \frac{e^{-\theta_1\left(\rho\tilde{\sigma}^2_{SA_n}+1\right)}\left(e^{-\theta_1R^2_{D_B}} - e^{-\theta_1R^2_{D_A}}\right)}{\theta_1\left(R^2_{D_A} - R^2_{D_B}\right)}. \quad (21)$$

Next, I_2 can be formulated by

$$I_2 = 1 - \Pr\left(\left|h\wedge_{BA}\right|^2 > \gamma_1\tilde{\sigma}^2_{BA} + \frac{\gamma_1\left(1 + d^2_{BA}\right)}{\rho}\right) = 1 - \frac{2e^{-\gamma_1\tilde{\sigma}^2_{BA}-\gamma_1/\rho}}{R^2_{D_A} - R^2_{D_B}}\int_{R_{D_B}}^{R_{D_A}} re^{-\gamma_1/\rho r^2}dr. \quad (22)$$

Similarly, I_2 can be expressed as follows:

$$I_2 = 1 - \frac{\rho e^{-\gamma_1\tilde{\sigma}^2_{BA}}}{\left(R^2_{D_A} - R^2_{D_B}\right)\gamma_1}\left(e^{-\gamma_1R^2_{D_A}/\rho} - e^{-\gamma_1R^2_{D_A}/\rho}\right). \quad (23)$$

Substituting (21) and (23) into (18), (17) is obtained.

It completes the proof.□ □

6. Throughput

In this section, we want to consider throughput performance. The throughput in delay-limited transmission mode is further investigated by considering outage probability computed in the previous section. At fixed rates R_1, R_2, the throughput can be examined by [13]

$$\mathcal{T} = (1 - P_{A,n})R_1 + (1 - P_{B,n})R_2. \quad (24)$$

7. Numerical Results

In this section, we present the numerical analysis of our NOMA system along with corroboration of analytical results. We set $|q_{n1}|^2 = 0.8$, $|q_{n2}|^2 = 0.2$, $R_{D_A} = 10$m, $R_{D_B} = 5$ m, $\tilde{\sigma}^2 = \tilde{\sigma}^2_{SA_n} = \tilde{\sigma}^2_{SB_n} = \tilde{\sigma}^2_{BA} = 0.001$, $R_1 = 0.5$, and $R_2 = 1$ bit per channel use.

Figure 2 depicts the outage probability versus transmit SNR at node *S*. As can be seen from Figure 2, the outage performance can be improved significantly at high SNR region. The outage performance of two groups of users is different. The main reason can be explained in two folds. First, different power allocation factors are assigned to two kinds of users. Secondly, signal detection is different when we examine it at

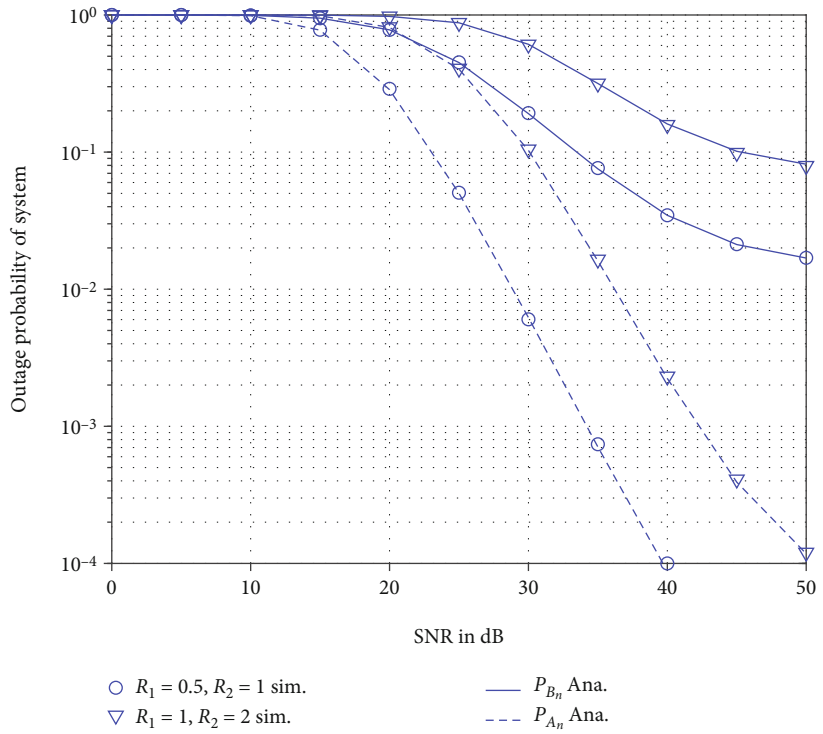

Figure 2: Outage probability of system versus SNR in dB varying $R_1 = R_2$.

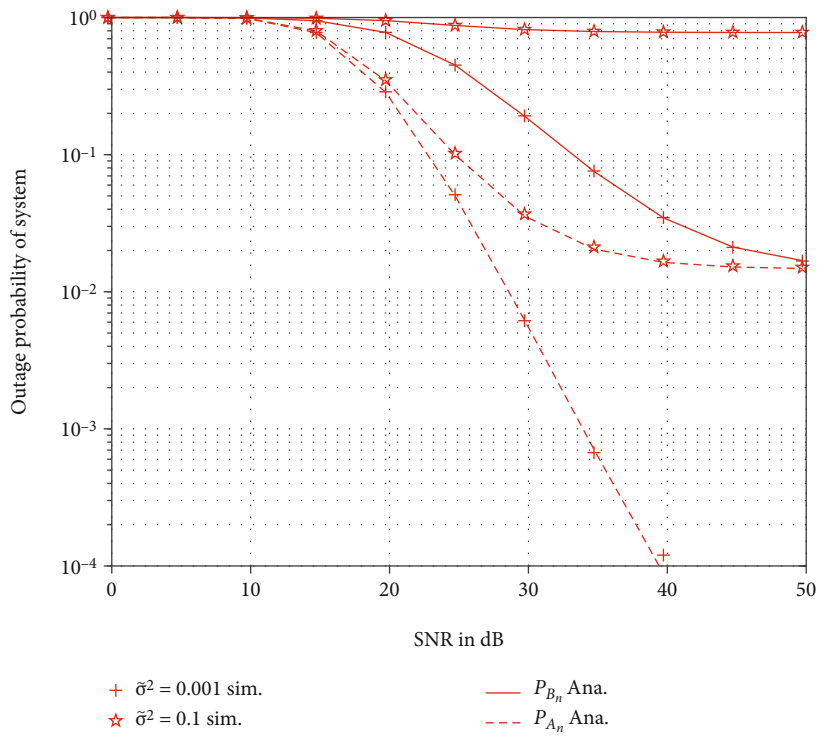

Figure 3: Outage probability of system versus SNR in dB varying $\tilde{\sigma}^2$.

each user B_n, A_n, while A_n is related to D2D link. We can conclude that higher required data rates R_1, R_2, result in worse outage performance.

The impact of channel error level to outage performance can be observed in Figure 3. Especially, the bad performance is seen for the case of $\tilde{\sigma}^2 = 0.1$. That means the exact channel

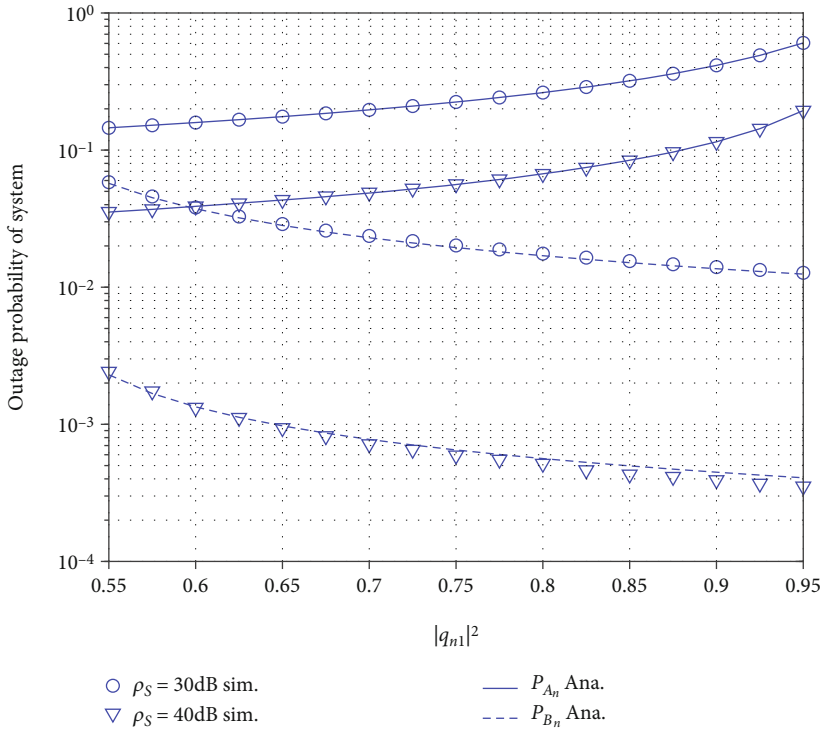

Figure 4: Outage probability of system versus $|q_{n1}|^2$ varying ρ_S.

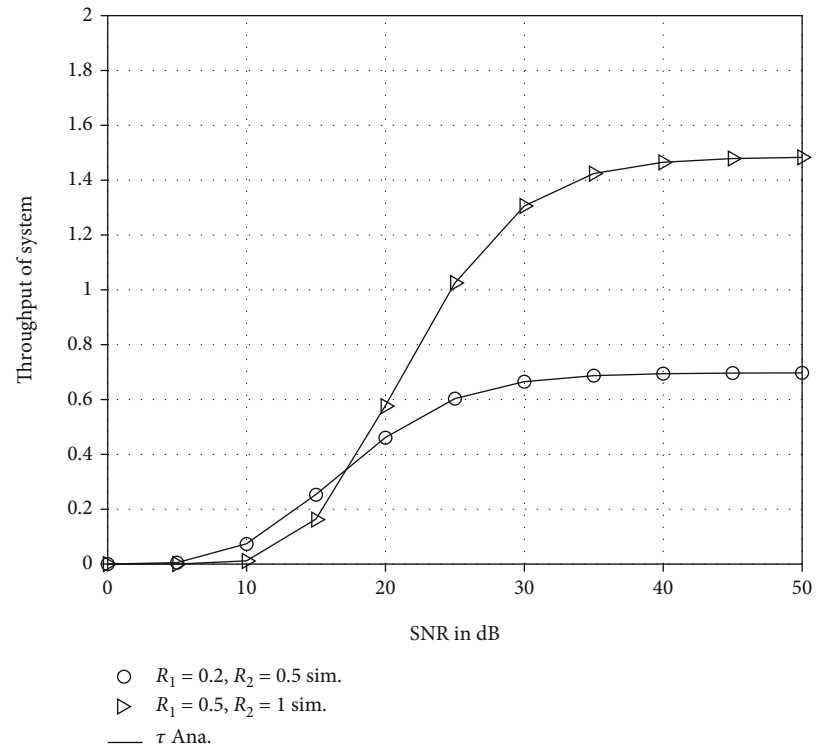

Figure 5: Throughput of system versus SNR in dB varying R_1 and R_2.

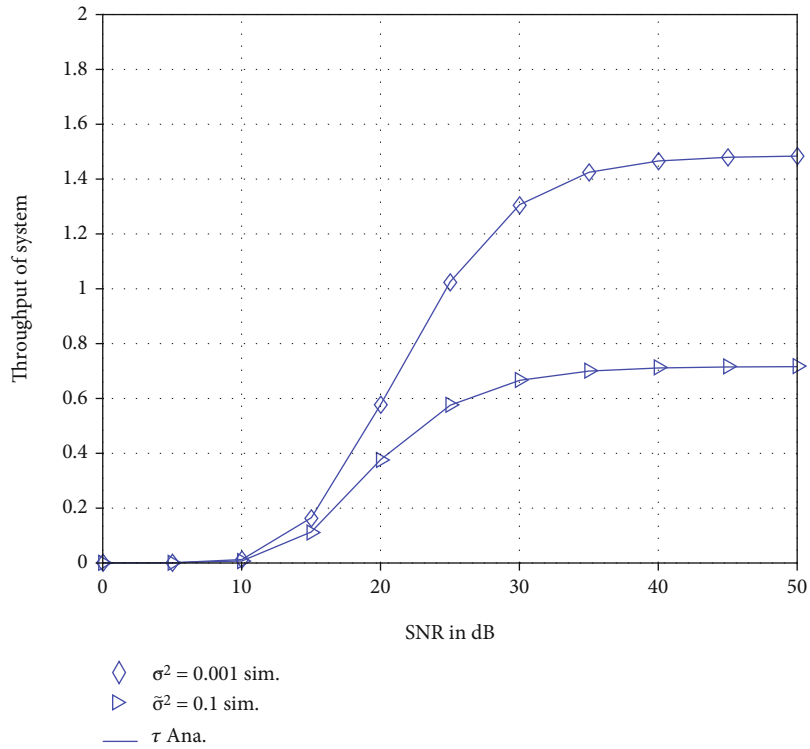

Figure 6: Throughput of system versus SNR in dB varying $\tilde{\sigma}^2$.

estimation plays an important role to keep outage performance at an acceptable level.

In Figure 4, we analyze outage probability versus power allocation $|q_{n1}|^2$ while varying ρ_S. For users in groups A_n and B_n, the best outage probability is achieved by $\rho_S = 40$d*B*. This shows the impact of base station transmit power and power allocation on the proposed system.

In Figure 5, we observe throughput versus SNR while varying the rates R_1 and R_2. The best throughput performance is achieved by lower R_1 and R_2 rates. Also, the throughput curves approach a ceiling in the high SNR region.

We can see the trend of throughput since it can be improved in the high SNR region, as shown in Figure 6. This figure confirms the role of channel error level to throughput performance. $\tilde{\sigma}^2 = 0.001$ and $\tilde{\sigma}^2 = 0.1$ are two values that result in a big gap of throughput when the value of SNR is greater than 35 dB.

8. Conclusions

We first reviewed previous contributions related to the design of NOMA for two groups of users in this article, and we then show expressions of outage probability for different kinds of users. To provide system performance analysis, we adopted a D2D and stochastic geometry to achieve the closed form expressions. We examine the system parameters to evaluate whether the outage performance can be enhanced. Compared among the cases of channel error levels, the proposed NOMA system can still perform despite the limitation of imperfect channel estimation. It is also worth noting that there may exist ceiling throughput at a high SNR region. In future work, we deploy multiple antennas at the source to further enhance performance at destinations.

Data Availability

No data were used to support this study.

Conflicts of Interest

The authors declare that they have no conflicts of interest.

References

[1] S. M. R. Islam, N. Avazov, O. A. Dobre, and K.-S. Kwak, "Power-domain non-orthogonal multiple access (NOMA) in 5G systems: potentials and challenges," *IEEE Communications Surveys & Tutorials*, vol. 19, no. 2, pp. 721–742, 2017.

[2] F. Zhou, Y. Wu, Y.-C. Liang, Z. Li, Y. Wang, and K.-K. Wong, "State of the art, taxonomy, and open issues on cognitive radio networks with NOMA," *IEEE Wireless Communications*, vol. 25, no. 2, pp. 100–108, 2017.

[3] S. M. R. Islam, M. Zeng, and O. A. Dobre, "NOMA in 5G systems: exciting possibilities for enhancing spectral efficiency," *IEEE 5G Tech Focus*, vol. 1, no. 2, pp. 1–6, 2017, http://5g.ieee.org/tech-focus.

[4] W. Hao, M. Zeng, Z. Chu, and S. Yang, "Energy-efficient power allocation in millimeter wave massive MIMO with non-orthogonal multiple access," *IEEE Wireless Communications Letters*, vol. 6, no. 6, pp. 782–785, 2017.

[5] F. Zhou, Y. Wu, R. Q. Hu, Y. Wang, and K.-K. Wong, "Energy-efficient NOMA enabled heterogeneous cloud radio access networks," *IEEE Network*, vol. 32, no. 2, pp. 152–160, 2018.

[6] S. Chen, B. Ren, Q. Gao, S. Kang, S. Sun, and K. Niu, "Pattern division multiple access—a novel nonorthogonal multiple access for fifthgeneration radio networks," *IEEE Transactions on Vehicular Technology*, vol. 66, no. 4, pp. 3185–3196, 2017.

[7] B. Zheng, M. Wen, F. Chen, J. Tang, and F. Ji, "Secure NOMA based full-duplex two-way relay networks with artificial noise against eavesdropping," in *IEEE International Conference on Communications (ICC)*, pp. 1–6, Kansas City, MO, USA, May 2018.

[8] Z. Ding, Y. Liu, J. Choi et al., "Application of non-orthogonal multiple access in LTE and 5G networks," *IEEE Communications Magazine*, vol. 55, no. 2, pp. 185–191, 2017.

[9] Z. Ding, M. Peng, and H. V. Poor, "Cooperative non-orthogonal multiple access in 5G systems," *IEEE Communications Letters*, vol. 19, no. 8, pp. 1462–1465, 2015.

[10] D. T. Do, M. S. Van Nguyen, M. Voznak, A. Kwasinski, and J. N. de Souza, "Performance analysis of clustering car-following V2X system with wireless power transfer and massive connections," *IEEE Internet of Things Journal*, 2021.

[11] D.-T. Do, M.-S. Van Nguyen, T.-A. Hoang, and B. M. Lee, "Exploiting joint base station equipped multiple antenna and full-duplex D2D users in power domain division based multiple access networks," *Sensors*, vol. 19, no. 11, p. 2475, 2019.

[12] A. S. Rajasekaran, O. Maraqa, H. U. Sokun, H. Yanikomeroglu, and S. Al-Ahmadi, "User clustering in mmWave-NOMA systems with user decoding capability constraints for B5G networks," *IEEE Access*, vol. 8, pp. 209949–209963, 2020.

[13] D. T. Do, A. T. Le, and B. M. Lee, "NOMA in cooperative underlay cognitive radio networks under imperfect SIC," *IEEE Access*, vol. 8, pp. 86180–86195, 2020.

[14] D.-T. Do, M.-S. V. Nguyen, F. Jameel, R. Jäntti, and I. S. Ansari, "erformance evaluation of relay-aided CR-NOMA for beyond 5G communications," *IEEE Access*, vol. 8, pp. 134838–134855, 2020.

[15] D.-T. Do, C.-B. Le, and F. Afghah, "Enabling full-duplex and energy harvesting in uplink and downlink of small-cell network relying on power domain based multiple access," *IEEE Access*, vol. 8, pp. 142772–142784, 2020.

[16] Y. Liu, Z. Ding, M. Elkashlan, and H. V. Poor, "Cooperative nonorthogonal multiple access with simultaneous wireless information and power transfer," *IEEE Journal on Selected Areas in Communications*, vol. 34, no. 4, pp. 938–953, 2016.

[17] S. Zhang, J. Liu, H. Guo, M. Qi, and N. Kato, "Envisioning device-to-device communications in 6G," *IEEE Network*, vol. 34, no. 3, pp. 86–91, 2020.

[18] J. Zhao, Y. Liu, K. K. Chai, Y. Chen, M. Elkashlan, and J. Alonso-Zarate, "NOMA-based D2D communications: towards 5G," in *2016 IEEE global communications conference (GLOBECOM)*, pp. 1–6, Washington, DC, USA, 2016.

[19] J. Zhao, Y. Liu, K. K. Chai, Y. Chen, and M. Elkashlan, "Joint subchannel and power allocation for NOMA enhanced D2D communications," *IEEE Transactions on Communications*, vol. 65, no. 11, pp. 5081–5094, 2017.

[20] Z. Zhang, Z. Ma, M. Xiao, Z. Ding, and P. Fan, "Full-duplex device-to-device-aided cooperative nonorthogonal multiple access," *IEEE Transactions on Vehicular Technology*, vol. 66, no. 5, pp. 4467–4471, 2017.

[21] X. Diao, J. Zheng, Y. Wu, and Y. Cai, "Joint computing resource, power, and channel allocations for D2D-assisted and NOMA-based mobile edge computing," *IEEE Access*, vol. 7, pp. 9243–9257, 2019.

[22] L. Pei, Z. Yang, C. Pan et al., "Energy-efficient D2D communications Underlaying NOMA-based networks with energy harvesting," *IEEE Communications Letters*, vol. 22, no. 5, pp. 914–917, 2018.

[23] Y. Pan, C. Pan, Z. Yang, and M. Chen, "Resource allocation for D2D communications underlaying a NOMA-based cellular network," *IEEE Wireless Communications Letters*, vol. 7, no. 1, pp. 130–133, 2018.

[24] M. M. Selim, M. Rihan, Y. Yang, L. Huang, Z. Quan, and J. Ma, "On the outage probability and power control of D2D underlaying NOMA UAV-assisted networks," *IEEE Access*, vol. 7, pp. 16525–16536, 2019.

[25] J. Kim, I. Lee, and J. Lee, "Capacity scaling for D2D aided cooperative relaying systems using NOMA," *IEEE Wireless Communications Letters*, vol. 7, no. 1, pp. 42–45, 2018.

[26] S. M. A. Kazmi, N. H. Tran, T. M. Ho, A. Manzoor, D. Niyato, and C. S. Hong, "Coordinated device-to-device communication with non-orthogonal multiple access in future wireless cellular networks," *IEEE Access*, vol. 6, pp. 39860–39875, 2018.

[27] H. Sun, Y. Xu, and R. Q. Hu, "A NOMA and MU-MIMO Supported Cellular Network with Underlaid D2D Communications," in *2016 IEEE 83rd Vehicular Technology Conference (VTC Spring)*, pp. 1–5, Nanjing, China, 2016.

[28] Z. Shi, S. Ma, H. ElSawy, G. Yang, and M. Alouini, "Cooperative HARQ-assisted NOMA scheme in large-scale D2D networks," *IEEE Transactions on Communications*, vol. 66, no. 9, pp. 4286–4302, 2018.

[29] Q. Li, P. Ren, and D. Xu, "Security enhancement and QoS provisioning for NOMA-based cooperative D2D networks," *IEEE Access*, vol. 7, pp. 129387–129401, 2019.

[30] Y. Jiang, L. Wang, H. Zhao, and H. -H. Chen, "Covert communications in D2D Underlaying cellular networks with power domain NOMA," *IEEE Systems Journal*, vol. 14, no. 3, pp. 3717–3728, 2020.

[31] I. Budhiraja, N. Kumar, S. Tyagi, S. Tanwar, and M. Guizani, "SWIPT-enabled D2D communication underlaying NOMA-based cellular networks in imperfect CSI," *IEEE Transactions on Vehicular Technology*, vol. 70, no. 1, pp. 692–699, 2021.

[32] Y. Xu, Z. Liu, Z. Yang, and C. Huang, "Energy-efficient resource allocation with imperfect CSI in NOMA-based D2D networks with SWIPT," in *2021 IEEE Wireless Communications and Networking Conference (WCNC)*, pp. 1–6, Nanjing, China, April 2021.

[33] J. Wang, X. Song, Y. Ma, and Z. Xie, "Power efficient secure full-duplex SWIPT using NOMA and D2D with imperfect CSI," *Sensors*, vol. 20, no. 18, p. 5395, 2020.

[34] T. Xing, N. Ma, and P. Zhang, "Two-stage power allocation for cooperative NOMA in D2D communications with imperfect CSI," in *2019 11th international conference on wireless communications and signal processing (WCSP)*, pp. 1–6, Xi'an, China, 2019.

[35] J. Wang, X. Song, L. Dong, and X. Han, "Power allocation for D2D aided cooperative NOMA system with imperfect CSI," *Wireless Networks*, 2021.

[36] R. Gupta, S. Tanwar, and N. Kumar, "Secrecy-ensured NOMA-based cooperative D2D-aided fog computing under

imperfect CSI," *Journal of Information Security and Applications*, vol. 59, article 102812, 2021.

[37] L. Tlebaldiyeva, G. Nauryzbayev, S. Arzykulov, Y. Akhmetkaziyev, M. S. Hashmi, and A. M. Eltawil, "A non-ideal NOMA-based mmwave D2D networks with hardware and CSI imperfections," 2020, http://arxiv.org/abs/2004.10506.

[38] D.-T. Do and A.-T. Le, "NOMA based cognitive relaying: transceiver hardware impairments, relay selection policies and outage performance comparison," *Computer Communications*, vol. 146, pp. 144–154, 2019.

[39] Z. Yang, Z. Ding, P. Fan, and G. K. Karagiannidis, "On the performance of non-orthogonal multiple access systems with partial channel information," *IEEE Transactions on Communications*, vol. 64, no. 2, pp. 654–667, 2016.

[40] Y. Ye, Y. Li, D. Wang, and G. Lu, "Power splitting protocol design for the cooperative NOMA with SWIPT," in *2017 IEEE International Conference on Communications (ICC)*, pp. 1–5, Paris, France, May 2017.

[41] I. S. Gradshteyn and I. M. Ryzhik, *Table of Integrals, Series, and Products*, Academic Press, San Diego, CA, 2000.

[42] H. Dang, M. Van Nguyen, D. Do, H. Pham, B. Selim, and G. Kaddoum, "Joint relay selection, full-duplex and device-to-device transmission in wireless powered NOMA networks," *IEEE Access*, vol. 8, pp. 82442–82460, 2020.